Supporting Information

Innovative Approach to Design SOFC Air Electrode Materials: High Entropy $La_{1-x}Sr_x(Co,Cr,Fe,Mn,Ni)O_{3-\delta}$ (x = 0, 0.1, 0.2, 0.3) Perovskites Synthesized by the Sol-gel Method

*Juliusz Dąbrowa**, *Anna Olszewska*, *Andreas Falkenstein*, *Christian Schwab*, *Maria Szymczak*, *Marek Zajusz*, *Maciej Możdzierz*, *Andrzej Mikuła*, *Klaudia Zielińska*, *Katarzyna Berent*, *Tomasz Czeppe*, *Manfred Martin*, *Konrad Świerczek*

Table S1. Parameters of the Rietveld refinement obtained for $La_{1-x}Sr_x(Co,Cr,Fe,Mn,Ni)O_{3-\delta}$ powders calcined at 700 °C for 6 h and cooled down with the furnace.

Sr content	*R*-3c structure					
x	*a* = *b* [Å]	error [Å]	*c* [Å]	error [Å]	R_{wp} [%]	GoF [-]
0	5.50855	0.00024	13.37122	0.00095	2.82	1.05
0.1	5.50518	0.00028	13.36259	0.00112	2.88	1.20
0.2	5.49968	0.00035	13.34638	0.00150	2.74	1.18
0.3	5.50625	0.00048	13.36189	0.00229	2.86	0.96
0.4	5.50666	0.00056	13.37229	0.00278	2.82	1.50
0.5	5.50493	0.00072	13.38037	0.00371	2.97	1.82

Table S2. Parameters of the Rietveld refinement obtained for $La_{1-x}Sr_x(Co,Cr,Fe,Mn,Ni)O_{3-\delta}$ pellets sintered at 1000 °C for 20 h.

x	phase	% wt.	*a* [Å]	error [Å]	*b* [Å]	error [Å]	*c* [Å]	error [Å]	Rwp [%]	GoF [-]
0	*Pnma*	100	5.46707	0.00011	7.74717	0.00017	5.51163	0.00011	7.17	2.01
0.1	*R*-3c	100	5.49665	0.00008			13.26755	0.00023	8.38	2.96
0.2	*R*-3c	100	5.48453	0.00014			13.27850	0.00039	7.38	2.33
0.3	*R*-3c	100	5.47375	0.00013			13.29138	0.00037	6.95	2.3
0.4	*R*-3c	94.2	5.46879	0.00016			13.30144	0.00048		
	R-3m	4.6	5.54197	0.00180			20.25243	0.00278	6.08	1.62
	Fm-3m	1.3	4.18251	0.00046						
0.5	*R*-3c	87.1	5.46482	0.00021			13.32241	0.00075		
	R-3m	10.6	5.58641	0.00056			20.23823	0.00339	6.23	1.98
	Fm-3m	2.3	4.18258	0.00023						

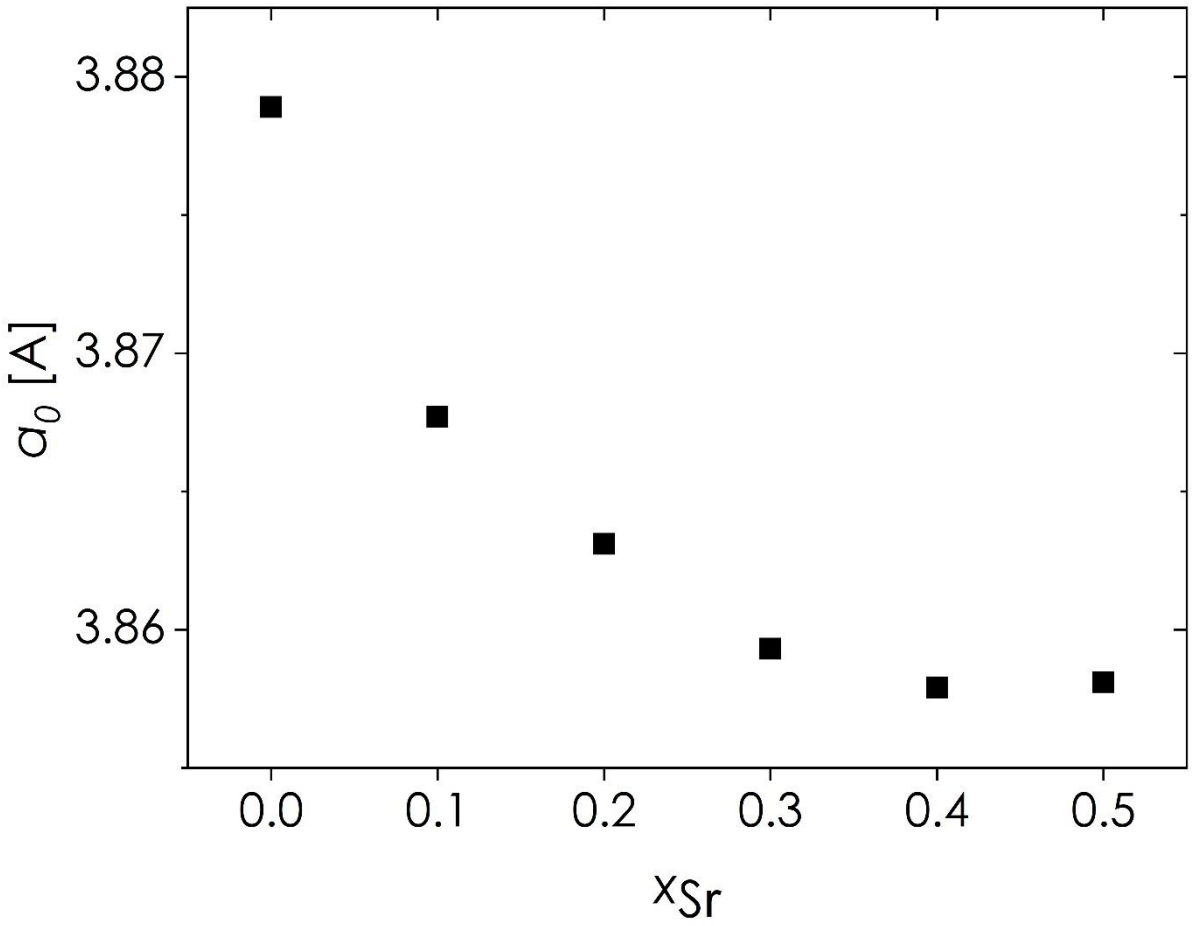

Figure S1. Normalized quasi-cubic unit cell parameter a_0 determined for the sintered $La_{1-x}Sr_x(Co,Cr,Fe,Mn,Ni)O_{3-\delta}$ samples as a function of Sr content.

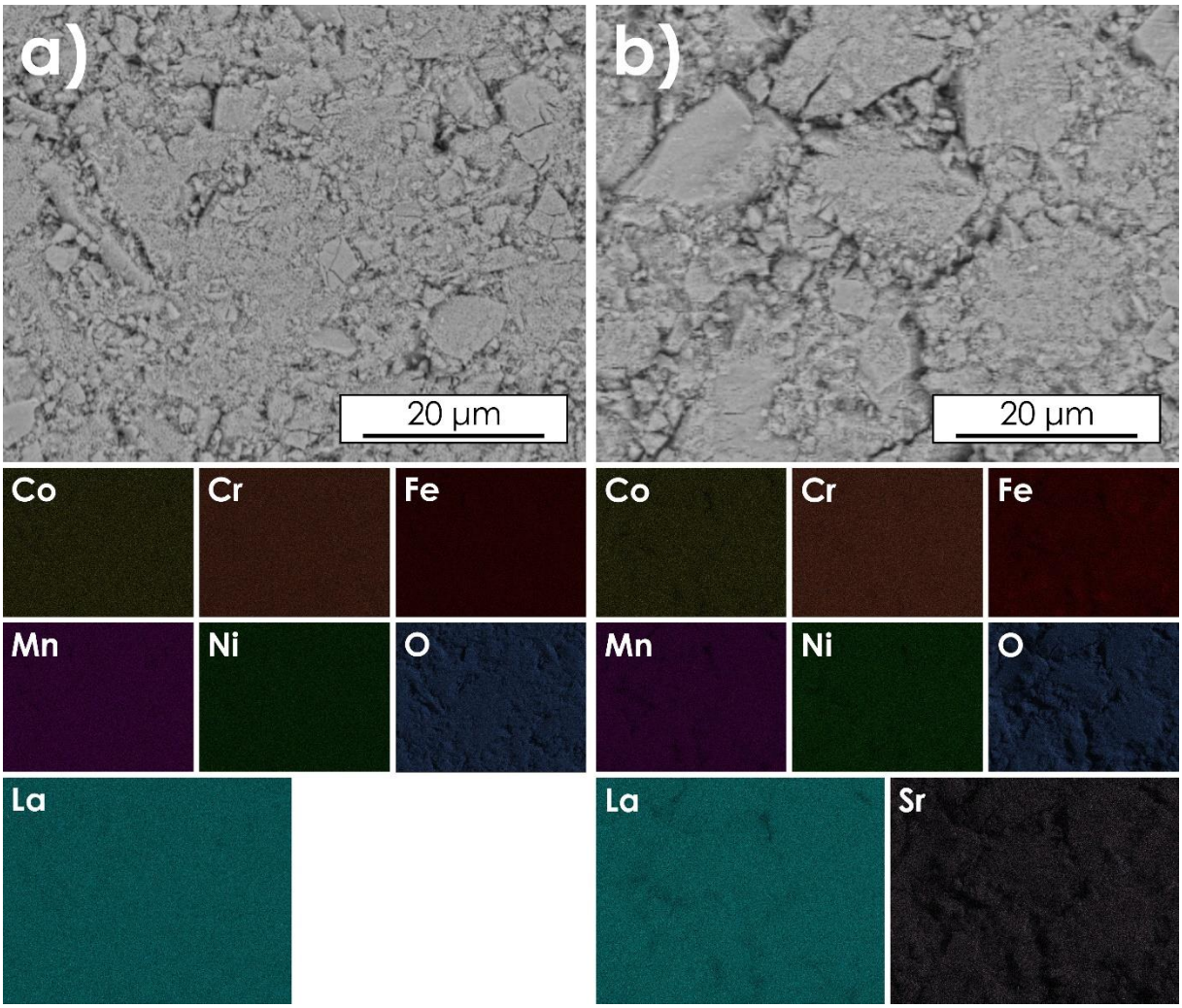

Figure S2. Results of EDS mappings of the air-quenched pellets sintered at 1000 °C for 20 h: a) La(Co,Cr,Fe,Mn,Ni)$O_{3-\delta}$, b) $La_{0.9}Sr_{0.1}$(Co,Cr,Fe,Mn,Ni)$O_{3-\delta}$.

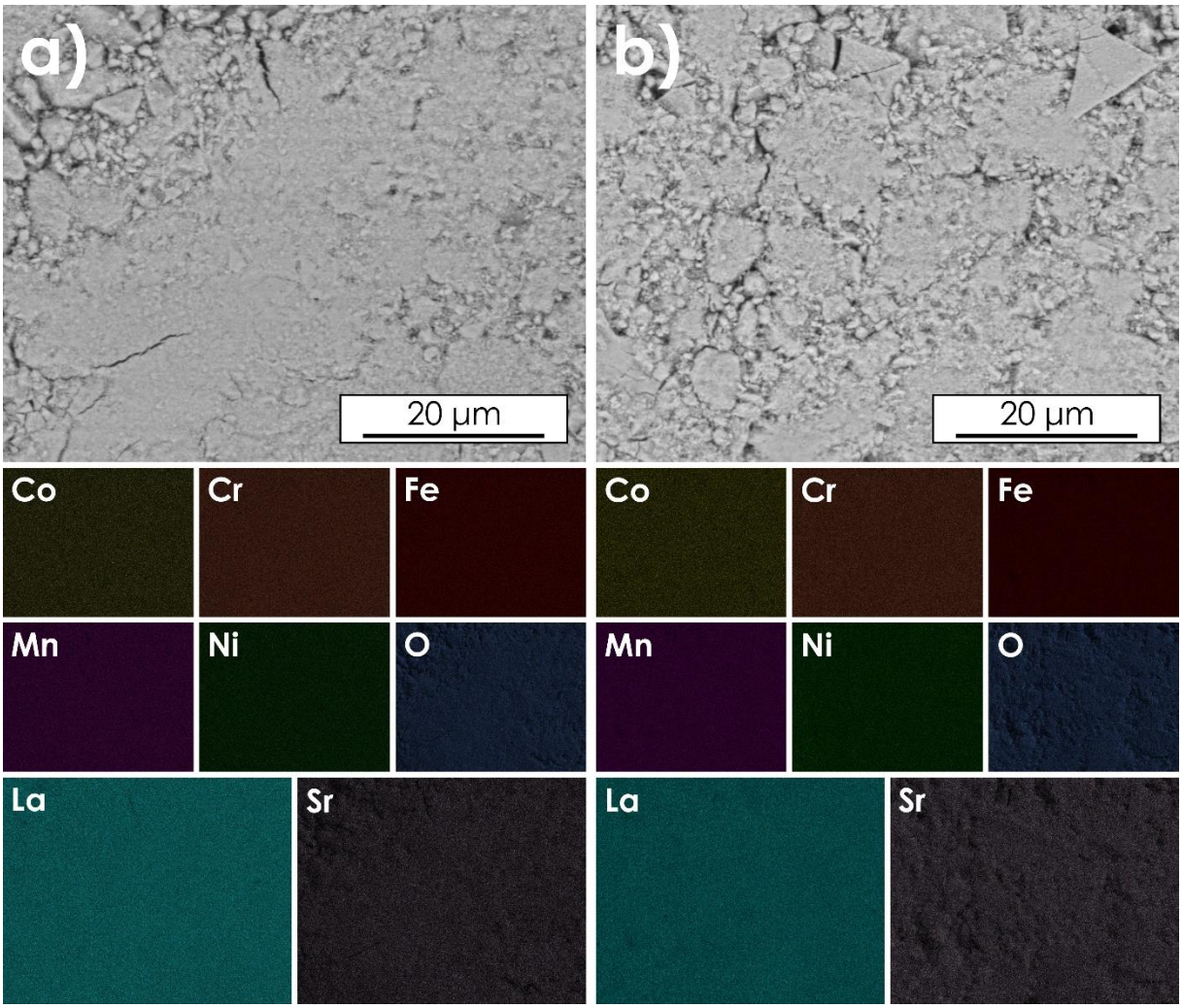

Figure S3. Results of EDS mappings of the air-quenched pellets sintered at 1000 °C for 20 h: a) $La_{0.8}Sr_{0.2}(Co,Cr,Fe,Mn,Ni)O_{3-\delta}$, b) $La_{0.7}Sr_{0.3}(Co,Cr,Fe,Mn,Ni)O_{3-\delta}$.

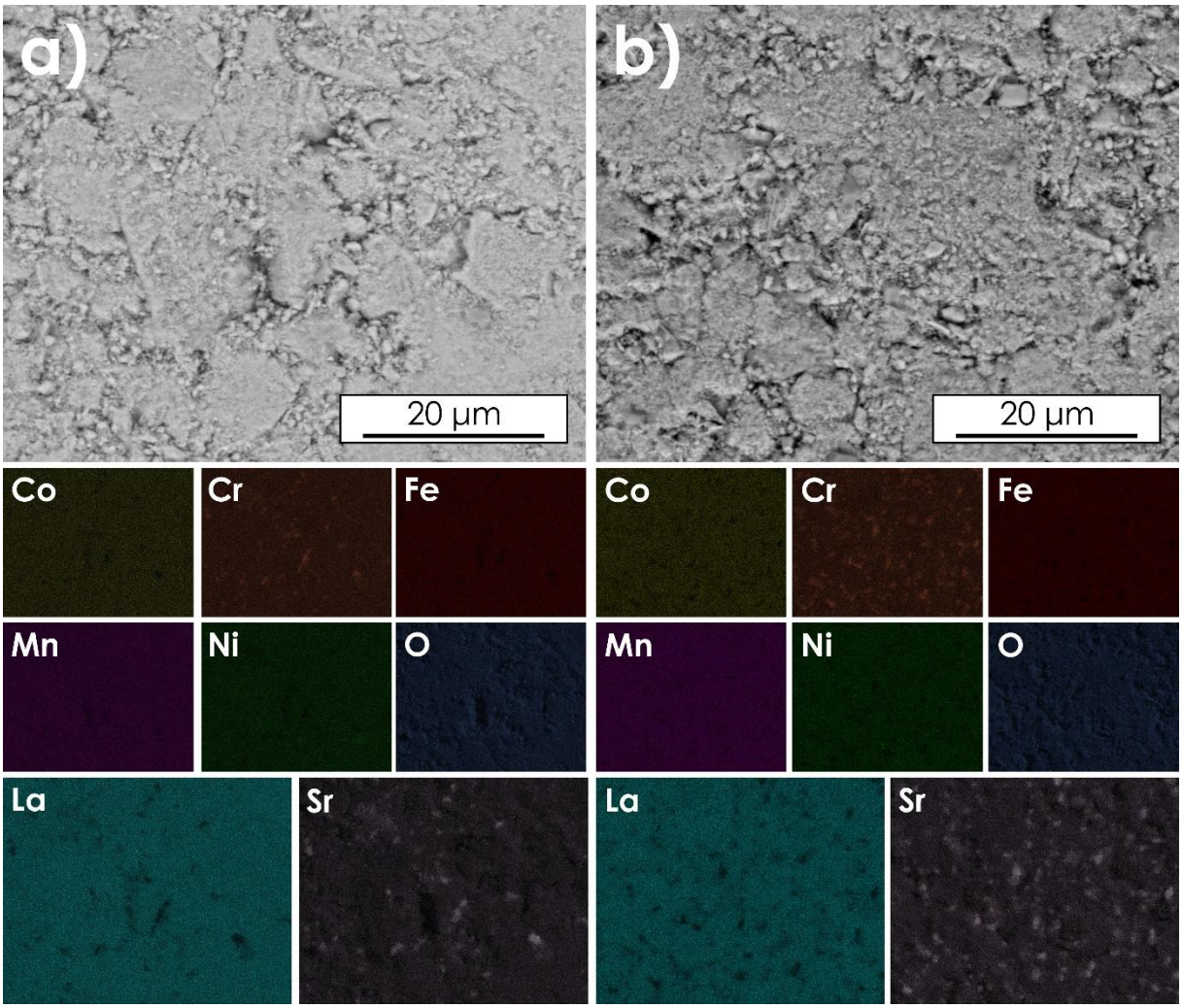

Figure S4. Results of EDS mappings of the air-quenched pellets sintered at 1000 °C for 20 h: a) $La_{0.6}Sr_{0.4}(Co,Cr,Fe,Mn,Ni)O_{3-\delta}$, b) $La_{0.5}Sr_{0.5}(Co,Cr,Fe,Mn,Ni)O_{3-\delta}$.

EDS quantitative analysis [at. %]

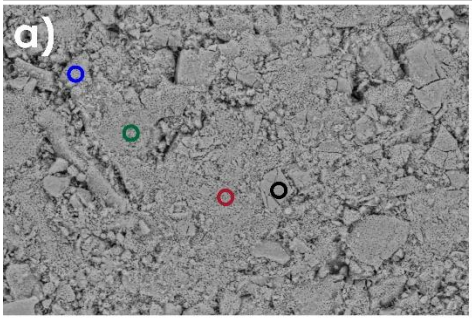

	La	Sr	Co	Cr	Fe	Mn	Ni	O
O	21.3	-	4.4	5.5	4.5	4.2	4.2	55.9
O	21.8	-	4.5	5.6	4.7	4.3	4.3	54.8
O	20.5	-	4.2	5.2	4.3	4.1	4.1	57.6
O	21.8	-	4.4	5.2	4.6	4.8	4.4	54.7

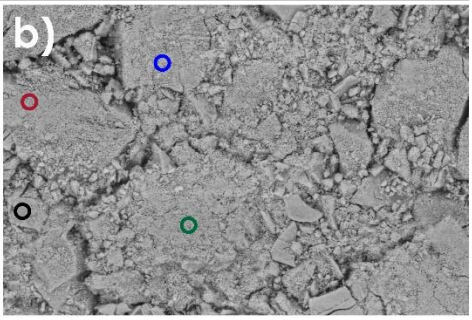

	La	Sr	Co	Cr	Fe	Mn	Ni	O
O	20.6	2.2	4.8	5.8	5.1	4.6	4.4	52.6
O	19.1	2.2	4.3	5.3	4.7	4.7	4.1	55.9
O	21.3	2.4	4.9	5.8	5.9	4.8	4.3	50.7
O	18.8	2.3	4.2	5.1	5.5	4.1	3.9	56.2

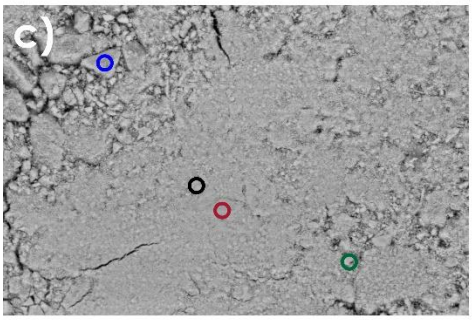

	La	Sr	Co	Cr	Fe	Mn	Ni	O
O	17.9	3.9	4.3	5.3	4.7	5.2	4.1	54.5
O	17.2	3.9	4.4	5.3	4.7	4.4	4.1	56.1
O	15.3	4.2	3.9	4.9	4.3	3.9	3.9	59.6
O	16.3	4.0	4.2	5.0	4.6	4.4	4.0	57.5

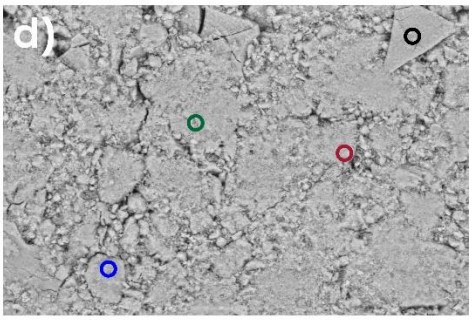

	La	Sr	Co	Cr	Fe	Mn	Ni	O
O	12.8	5.8	4.2	4.4	4.0	3.8	3.9	61.2
O	13.6	5.5	4.4	4.8	4.3	4.0	4.2	59.1
O	13.5	5.7	4.3	4.6	4.2	3.9	3.7	60.0
O	13.8	5.4	4.4	4.6	4.2	4.0	3.7	59.7

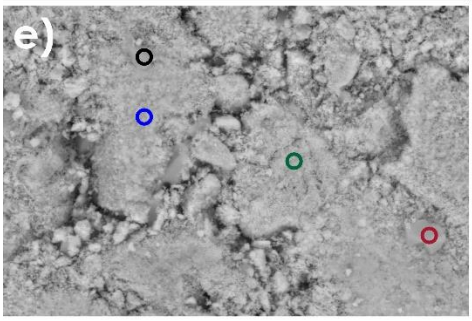

	La	Sr	Co	Cr	Fe	Mn	Ni	O
O	5.7	15.2	1.9	10.9	1.9	1.9	1.7	60.7
O	4.4	18.8	1.6	13.7	1.7	1.7	2.2	55.9
O	15.0	7.6	5.2	5.5	5.4	5.0	4.5	51.8
O	14.7	8.1	5.0	5.9	5.1	4.8	4.7	51.6

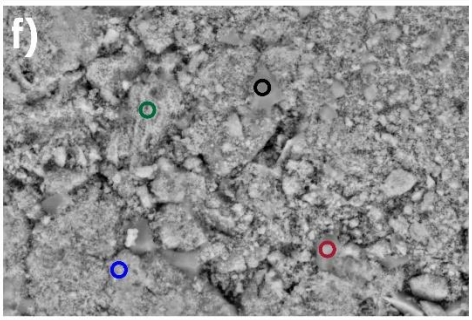

	La	Sr	Co	Cr	Fe	Mn	Ni	O
O	4.4	20.0	1.8	14.0	1.9	1.9	1.7	54.3
O	3.7	16.5	1.5	11.2	1.6	1.6	1.4	62.3
O	12.6	9.0	5.5	5.1	5.4	5.1	5.7	51.6
O	12.5	9.0	5.2	4.6	5.4	5.2	4.9	53.2

Figure S5. Results of the EDS point analysis of pellets sintered at 1000 °C for 20h: a) La(Co,Cr,Fe,Mn,Ni)$O_{3-\delta}$ b) $La_{0.9}Sr_{0.1}$(Co,Cr,Fe,Mn,Ni)$O_{3-\delta}$ c) $La_{0.8}Sr_{0.2}$(Co,Cr,Fe,Mn,Ni)$O_{3-\delta}$ d) $La_{0.7}Sr_{0.3}$(Co,Cr,Fe,Mn,Ni)$O_{3-\delta}$ e) $La_{0.6}Sr_{0.4}$(Co,Cr,Fe,Mn,Ni)$O_{3-\delta}$ f) $La_{0.5}Sr_{0.5}$(Co,Cr,Fe,Mn,Ni)$O_{3-\delta}$

Table S3. The average compositions of $La_{1-x}Sr_x(Co,Cr,Fe,Mn,Ni)O_{3-\delta}$ determined by the EDS area analysis. The normalized values (with respect to the A-site positions, $x_{La} + x_{Sr} = 1$) are also provided.

Content [at. %]							
Nominal	La	Sr	Co	Cr	Fe	Mn	Ni
0	22.9(5)	-	4.6(3)	6.0(2)	4.8(3)	4.3(2)	4.4(3)
0.1	20.8(5)	2.1(2)	4.6(3)	6.0(2)	5.2(3)	4.4(3)	4.4(3)
0.2	18.4(4)	3.8(3)	4.7(3)	5.7(2)	4.9(3)	4.6(2)	4.6(3)
0.3	16.4(4)	5.5(3)	5.3(3)	5.7(2)	5.0(3)	4.8(2)	4.7(3)
0.4	13.8(3)	7.7(4)	4.9(3)	5.5(2)	4.9(2)	4.7(2)	4.6(3)
0.5	13.80	11.30	3.60	3.60	3.60	3.60	3.40
Normalized content ($x_{La}+x_{Sr}$) = 1							
Nominal	La	Sr	Co	Cr	Fe	Mn	Ni
0	1.00	-	0.20	0.26	0.21	0.19	0.19
0.1	0.91	0.09	0.20	0.26	0.23	0.19	0.19
0.2	0.83	0.17	0.21	0.26	0.22	0.21	0.21
0.3	0.75	0.25	0.24	0.26	0.23	0.22	0.21
0.4	0.64	0.36	0.23	0.26	0.23	0.22	0.21
0.5	0.55	0.45	0.14	0.14	0.14	0.14	0.14

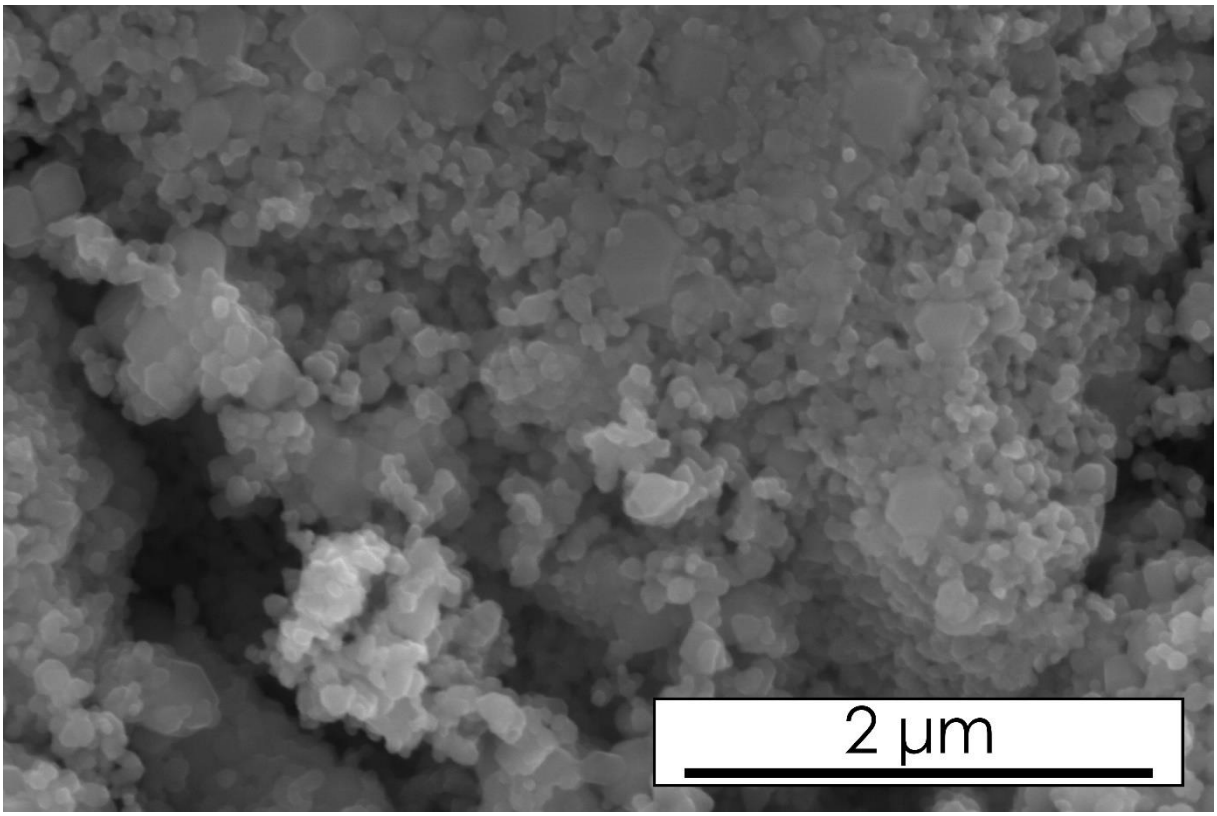

Figure S6. High magnification of the surface of the $La_{0.7}Sr_{0.3}(Co,Cr,Fe,Mn,Ni)O_{3-\delta}$ pellet sintered at 1000 °C for 20h.

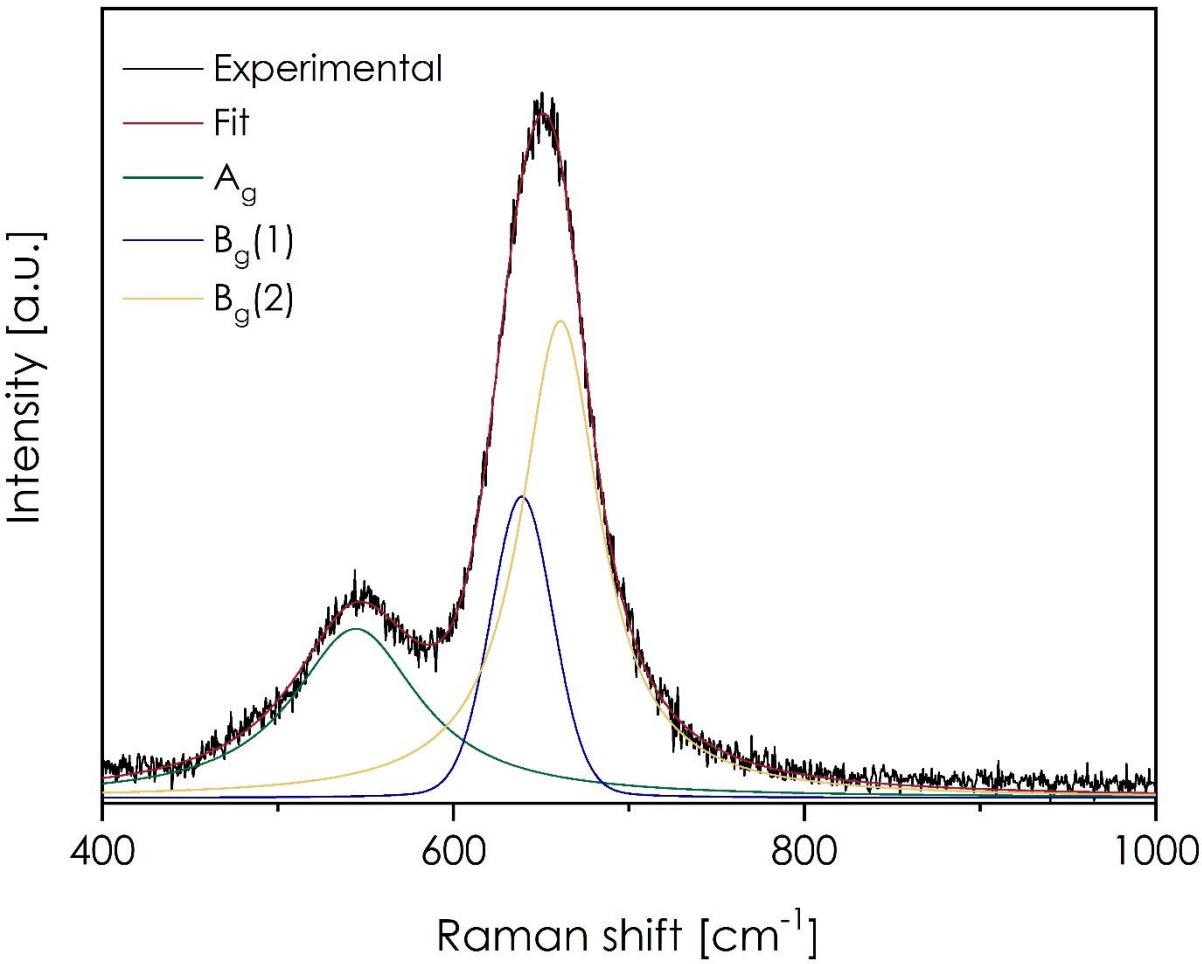

Figure S7. Exemplary deconvolution of the Raman spectra measured for the La(Co,Cr,Fe,Mn,Ni)$O_{3-\delta}$.

Table S4. Determined positions of the Raman main bands for the $La_{1-x}Sr_x$(Co,Cr,Fe,Mn,Ni)$O_{3-\delta}$ materials:

x	A_g [cm^{-1}]	B_g [cm^{-1}]
0	547	650
0.1	549	659
0.2	548	663
0.3	548	663
0.4	552	668
0.5	549	666

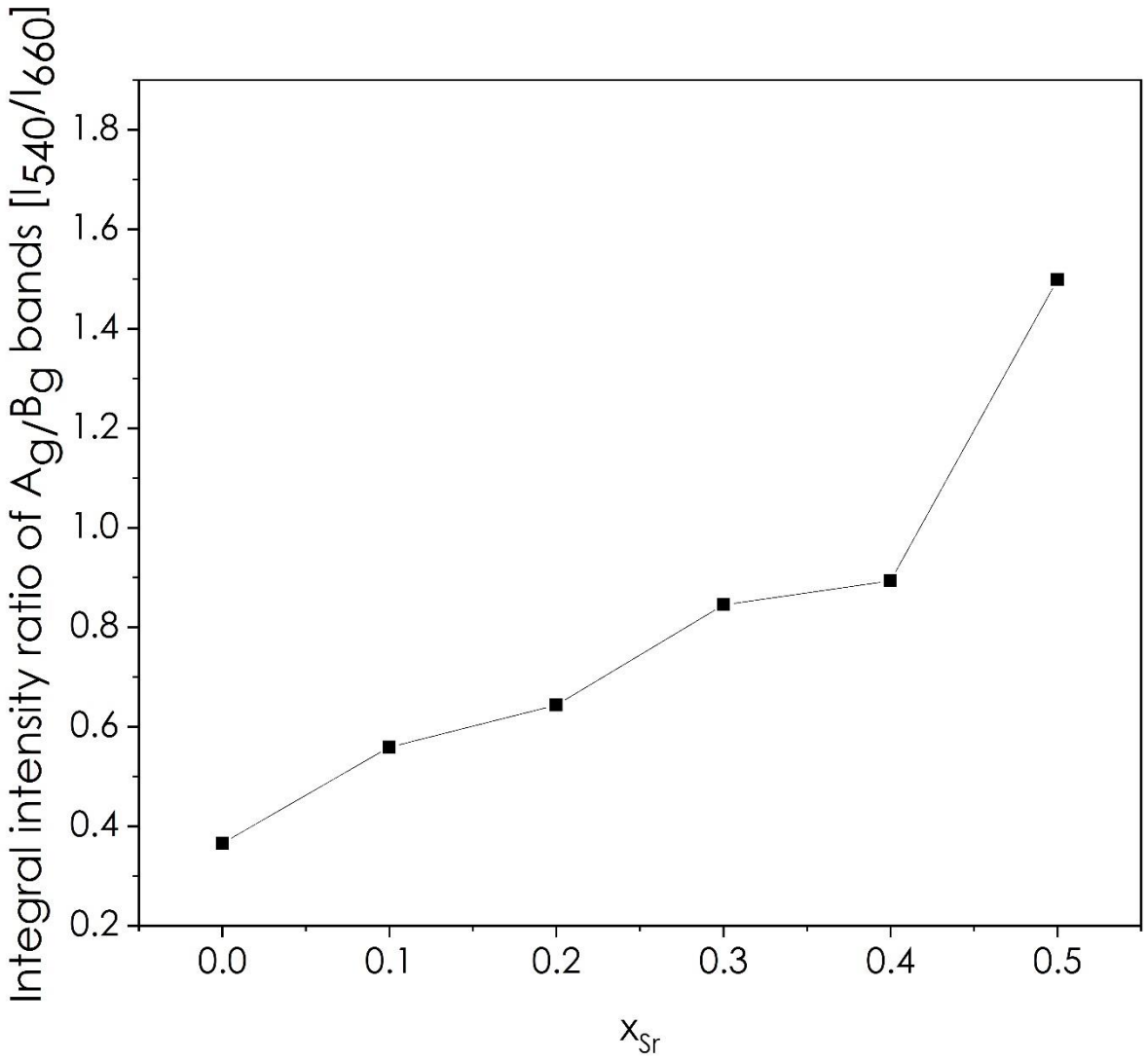

Figure S8. Integral intensities ratio of A_g and B_g bands (see Figure S6), correlated with the relative oxygen vacancy ratio.

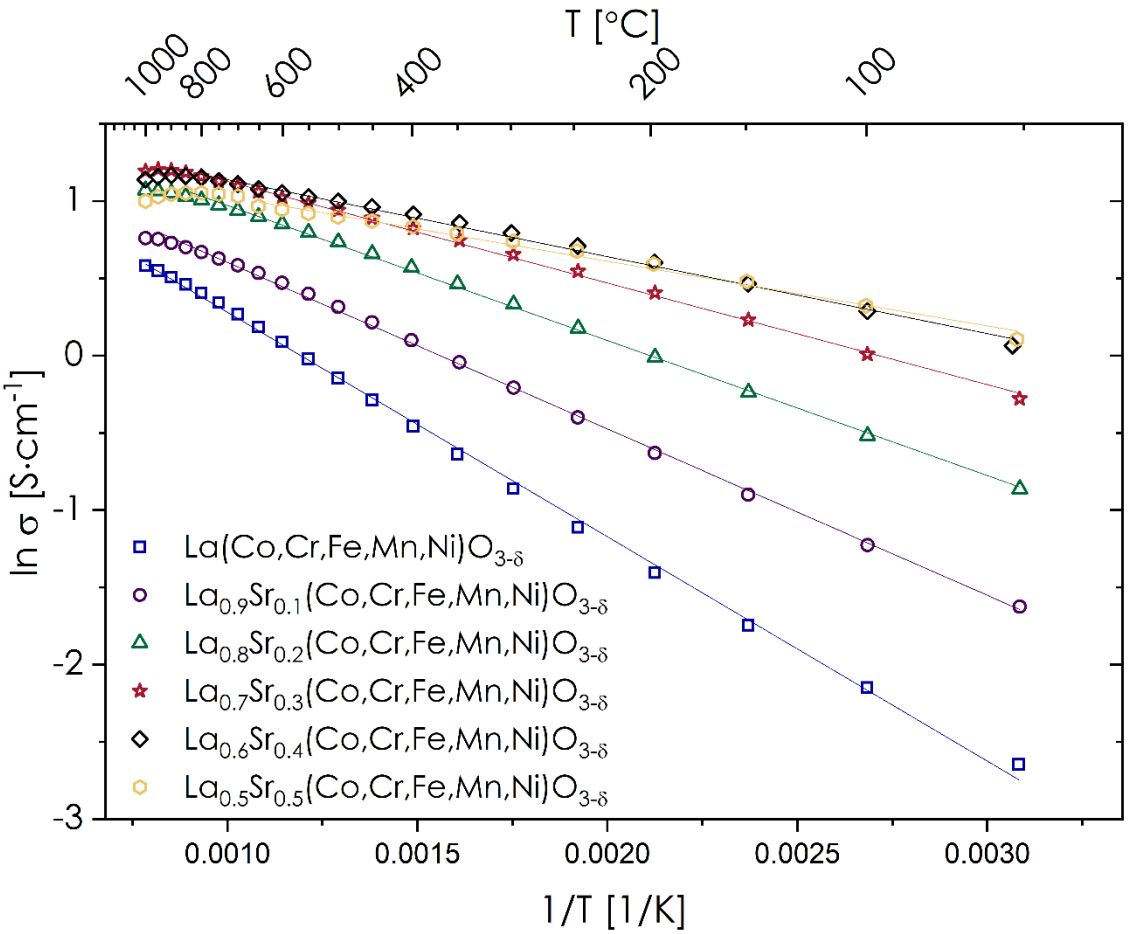

Figure S9. Total electrical conductivity of all studied LSTM materials (including multiphase ones) as obtained by the EIS measurements.

Table S5. Activation energies E_a determined for the LSTM materials from the linear parts of the electrical conductivity Arrhenius plots. The maximum values of the conductivity σ_{max}, together with their respective temperatures T_{max} are also provided.

Composition	E_a [eV]	Temperature range [°C]	σ_{max} [S cm^{-1}]	T_{max} [°C]
La(Co,Cr,Fe,Mn,Ni)$O_{3-\delta}$	0.288(3)	25-1000	3.82	1000
$La_{0.9}Sr_{0.1}$(Co,Cr,Fe,Mn,Ni)$O_{3-\delta}$	0.214(2)	25 - 950	5.76	1000
$La_{0.8}Sr_{0.2}$(Co,Cr,Fe,Mn,Ni)$O_{3-\delta}$	0.173(1)	25 - 850	11.76	1000
$La_{0.7}Sr_{0.3}$(Co,Cr,Fe,Mn,Ni)$O_{3-\delta}$	0.131(1)	25 - 850	16.03	950
$La_{0.6}Sr_{0.4}$(Co,Cr,Fe,Mn,Ni)$O_{3-\delta}$	0.099(2)	25 - 800	14.65	900
$La_{0.5}Sr_{0.5}$(Co,Cr,Fe,Mn,Ni)$O_{3-\delta}$	0.083(2)	25 - 650	11.32	800

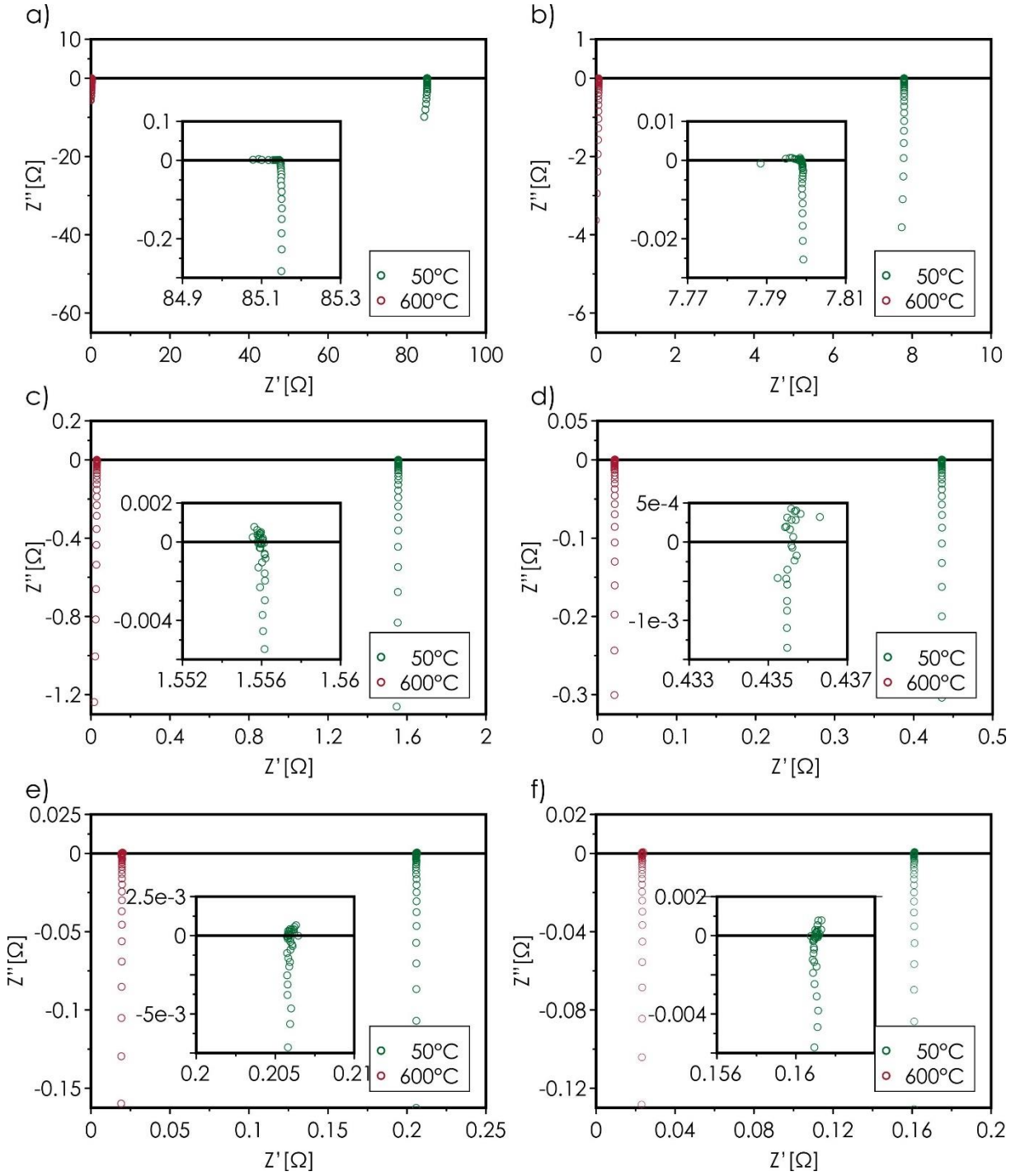

Figure S10. Exemplary EIS spectra measured for the $La_{1-x}Sr_x(Co,Cr,Fe,Mn,Ni)O_{3-\delta}$ materials: a) $La(Co,Cr,Fe,Mn,Ni)O_{3-\delta}$ b) $La_{0.9}Sr_{0.1}(Co,Cr,Fe,Mn,Ni)O_{3-\delta}$ c) $La_{0.8}Sr_{0.2}(Co,Cr,Fe,Mn,Ni)O_{3-\delta}$ d) $La_{0.7}Sr_{0.3}(Co,Cr,Fe,Mn,Ni)O_{3-\delta}$ e) $La_{0.6}Sr_{0.4}(Co,Cr,Fe,Mn,Ni)O_{3-\delta}$ f) $La_{0.5}Sr_{0.5}(Co,Cr,Fe,Mn,Ni)O_{3-\delta}$

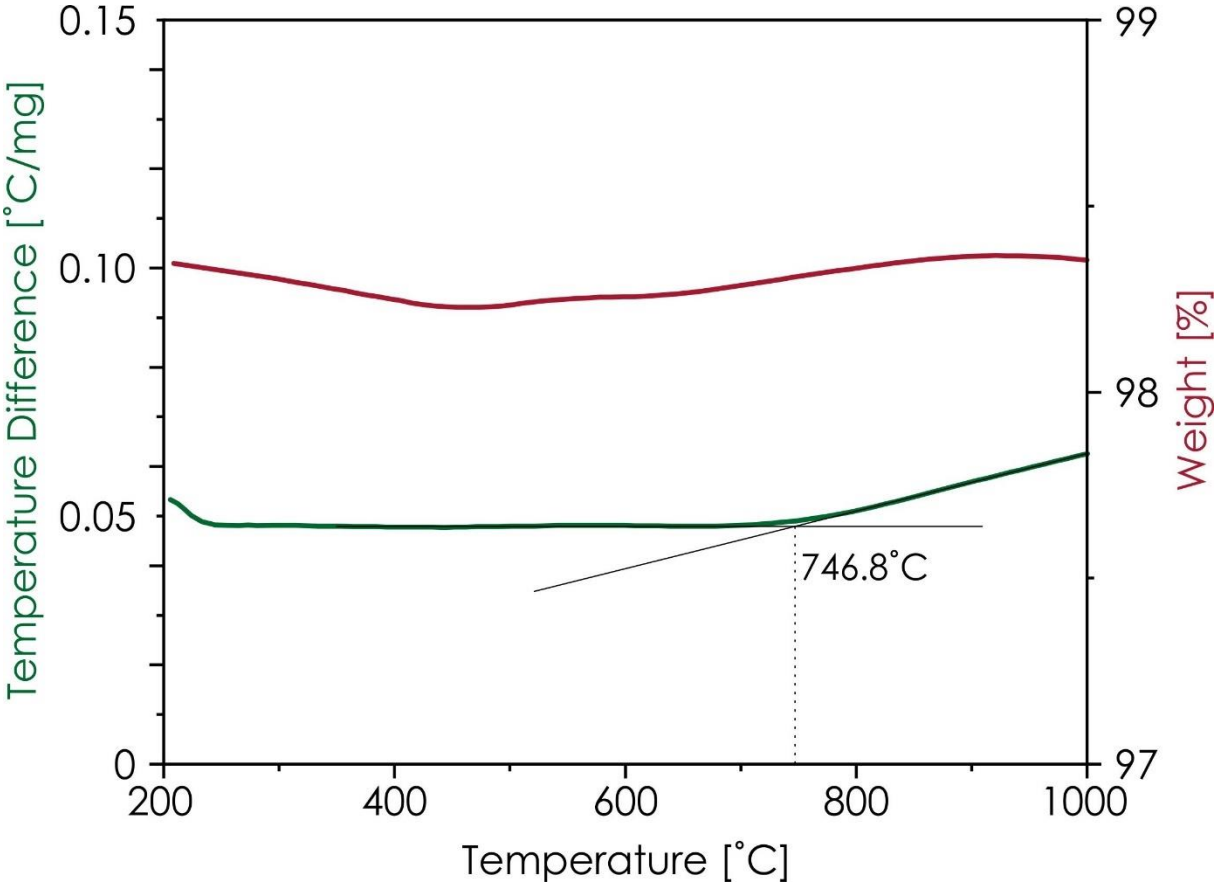

Figure S11. Results of the DTA-TG measurement conducted in air atmosphere for the $La_{0.7}Sr_{0.3}(Co,Cr,Fe,Mn,Ni)O_{3-\delta}$. Data collected for the heating during the second subsequent heating-cooling run for the as-calcined powder.

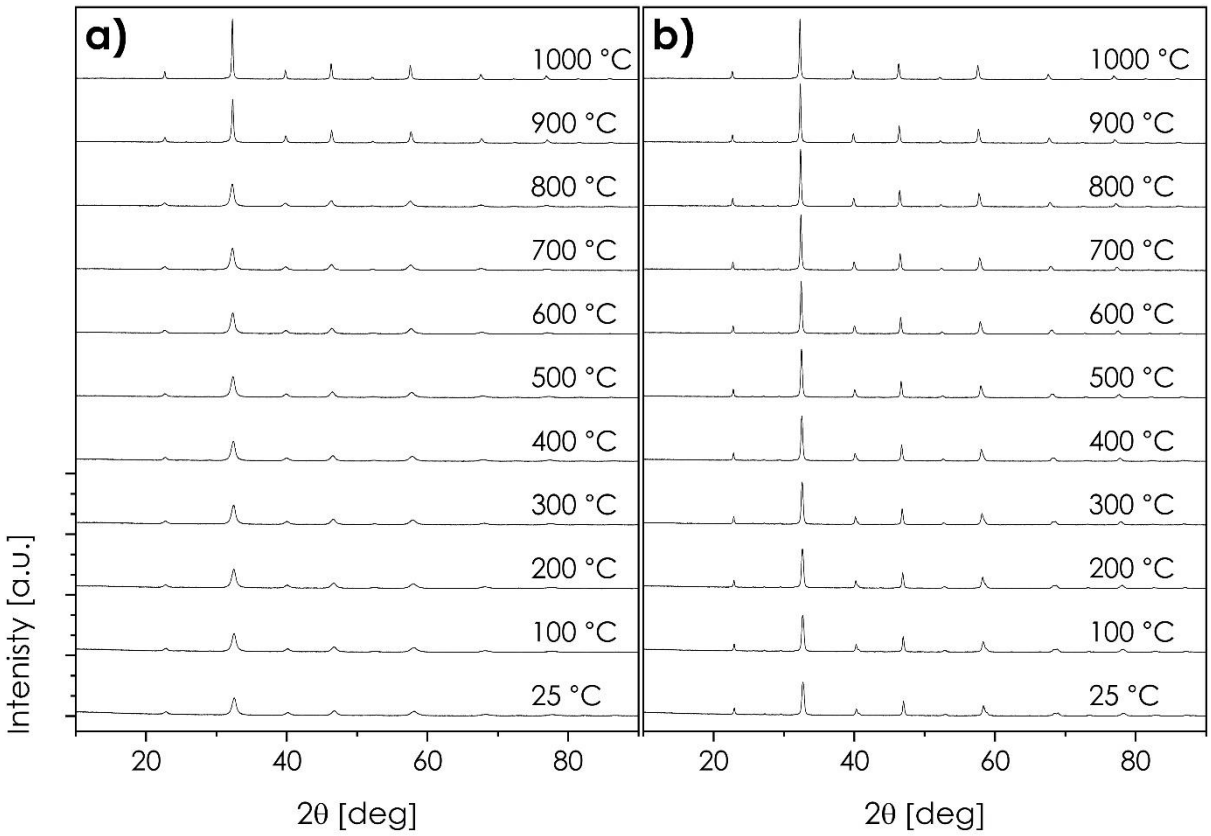

Figure S12. The diffractograms obtained from the *in-situ* high-temperature XRD measurements performed on the calcined $La_{0.7}Sr_{0.3}(Co,Cr,Fe,Mn,Ni)O_{3-\delta}$ powder: a) upon heating b) upon cooling.

Table S6. Parameters of the Rietveld refinement obtained for the $La_{0.7}Sr_{0.3}(Co,Cr,Fe,Mn,Ni)O_{3-\delta}$ powder calcined at 700 °C for 6 h and cooled down with the furnace, studied *in-situ* with the use of HT XRD.

Heating										
	Pm-3m				***R-3c***					
T [°C]	***a* [Å]**	**error [Å]**	**Rwp [%]**	**GoF [-]**	***a* = *b* [Å]**	**error [Å]**	***c* [Å]**	**error [Å]**	**R_{wp} [%]**	**GoF [-]**
1000	3.92082	0.00007	3.17	1.19	5.54395	0.00048	13.57177	0.00243	3.05	1.10
900	3.91463	0.00009	3.07	1.12	5.53278	0.00077	13.56136	0.00401	3.52	1.47
800	3.92350	0.00021	2.91	1.00	5.55545	0.00050	13.53135	0.00254	2.81	0.93
700	3.91574	0.00022	2.87	0.98	5.55457	0.00063	13.53945	0.00322	2.83	0.96
600	-	-	-	-	5.54227	0.00058	13.49309	0.00292	2.90	1.00
500	-	-	-	-	5.53058	0.00047	13.44328	0.00227	2.27	0.98
400	-	-	-	-	5.52979	0.00052	13.43948	0.00254	2.97	1.05
300	-	-	-	-	5.52579	0.00047	13.41928	0.00225	2.86	0.97
200	-	-	-	-	5.51489	0.00049	13.39092	0.00237	2.90	0.99
100	-	-	-	-	5.50900	0.00051	13.37916	0.00256	2.87	0.97
25	-	-	-	-	5.50625	0.00048	13.36189	0.00229	2.86	0.96
Cooling										
	Pm-3m				***R-3c***					
T [°C]	***a* [Å]**	**error [Å]**	**R_{wp} [%]**	**GoF [-]**	***a* = *b* [Å]**	**error [Å]**	***c* [Å]**	**error [Å]**	**R_{wp} [%]**	**GoF [-]**
1000	3.92082	0.00007	3.17	1.19	5.54395	0.00048	13.57177	0.00243	3.05	1.10
900	3.91268	0.00007	3.12	1.15	5.53454	0.00031	13.57043	0.00157	3.26	1.25
800	3.90806	0.00007	3.29	1.28	5.53127	0.00013	13.51614	0.00060	3.21	1.22
700	3.90150	0.00008	3.40	1.36	5.52361	0.00013	13.48383	0.00052	3.17	1.18
600	-	-	-	-	5.51462	0.00012	13.44807	0.00045	3.22	1.21
500	-	-	-	-	5.50751	0.00012	13.41966	0.00041	3.14	1.13
400	-	-	-	-	5.50231	0.00012	13.39680	0.00042	3.26	2.22
300	-	-	-	-	5.49323	0.00013	13.36406	0.00043	3.40	1.33
200	-	-	-	-	5.48592	0.00013	13.33536	0.00043	3.36	1.27
100	-	-	-	-	5.48090	0.00015	13.31147	0.00046	3.49	1.36
25	-	-	-	-	5.47697	0.00015	13.29466	0.00046	3.51	1.38

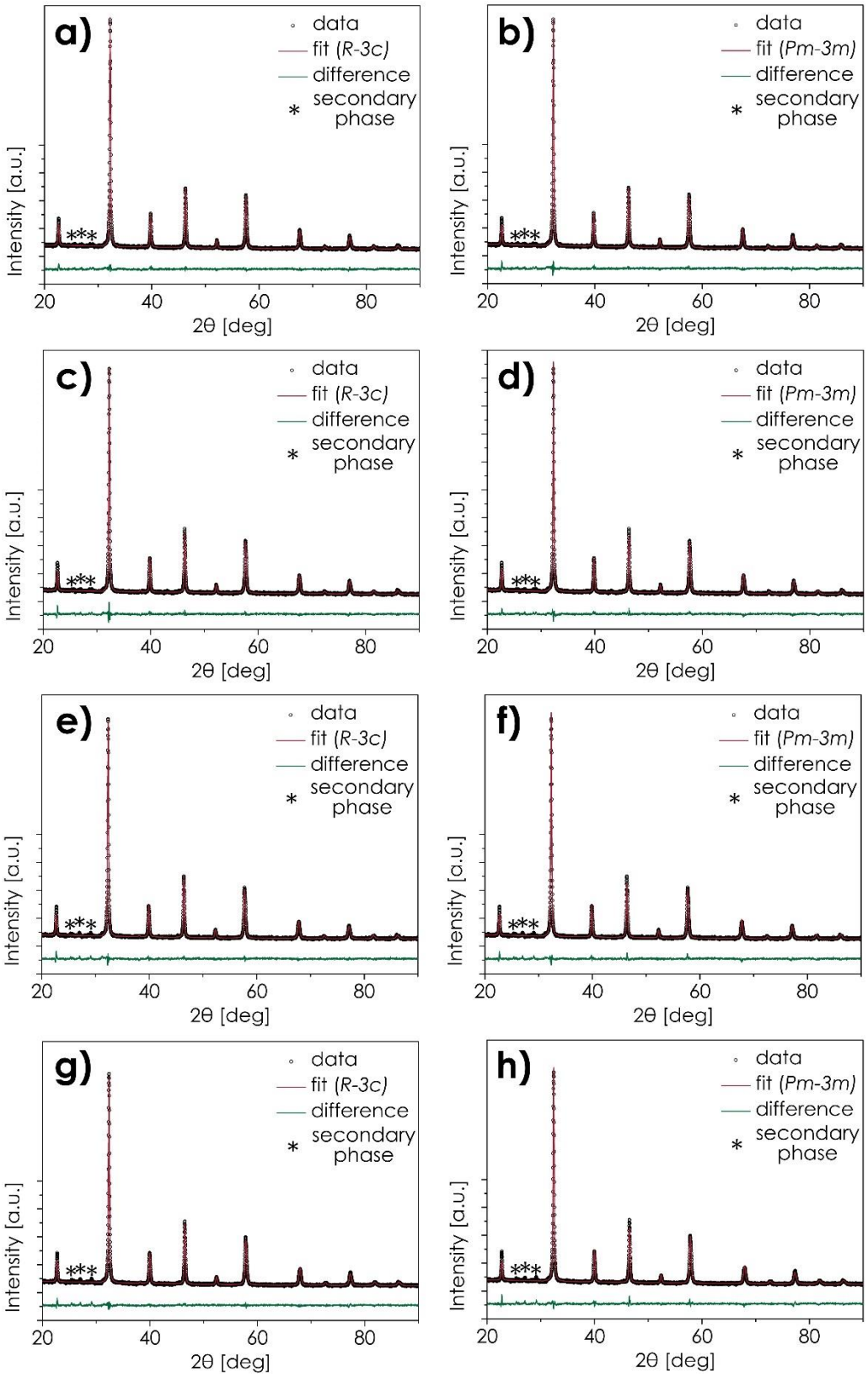

Figure S13. Exemplary results of Rietveld refinement for the high-temperature in-situ diffractograms of the $La_{0.7}Sr_{0.3}(Co,Cr,Fe,Mn,Ni)O_{3-\delta}$ obtained for: a) 1000 °C assuming *R*-3*c* symmetry b) 1000 °C assuming *Pm*-3*m* symmetry c) 900 °C assuming *R*-3*c* symmetry d) 900 °C assuming *Pm*-3*m* symmetry e) 800 °C assuming *R*-3*c* symmetry f) 800 °C assuming *Pm*-3*m* symmetry g) 700 °C assuming *R*-3*c* symmetry h) 700 °C assuming *Pm*-3*m* symmetry.

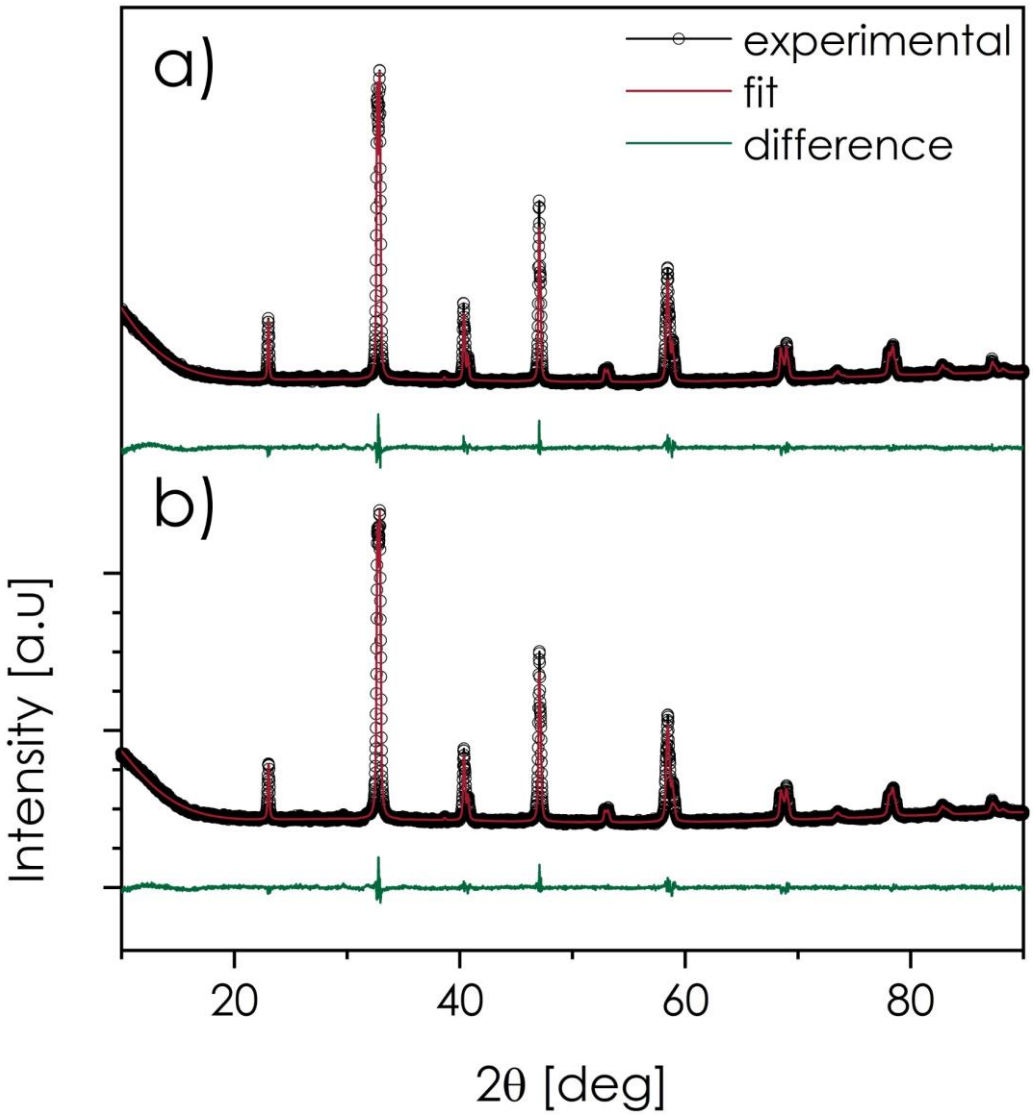

Figure S14. Diffraction patterns obtained for the $La_{0.7}Sr_{0.3}(Co,Cr,Fe,Mn,Ni)O_{3-\delta}$ pellet: a) after additional heat treatment at 1000 °C for 100 hours; b) before additional heat treatment.

Table S7. Structural parameters and Rietveld residuals for the *R*-3*c*-structured, single-phase $La_{0.7}Sr_{0.3}(Co,Cr,Fe,Mn,Ni)O_{3-\delta}$ sample before and after additional treatment at 1000 °C for 100 hours.

	***a* = *b* [Å]**	**error [Å]**	***c* [Å]**	**error [Å]**	**R_{wp} [%]**	**GoF [-]**
before	5.47480	0.00010	13.28856	0.00030	2.91	1.45
after	5.47451	0.00009	13.28462	0.00026	3.11	1.70

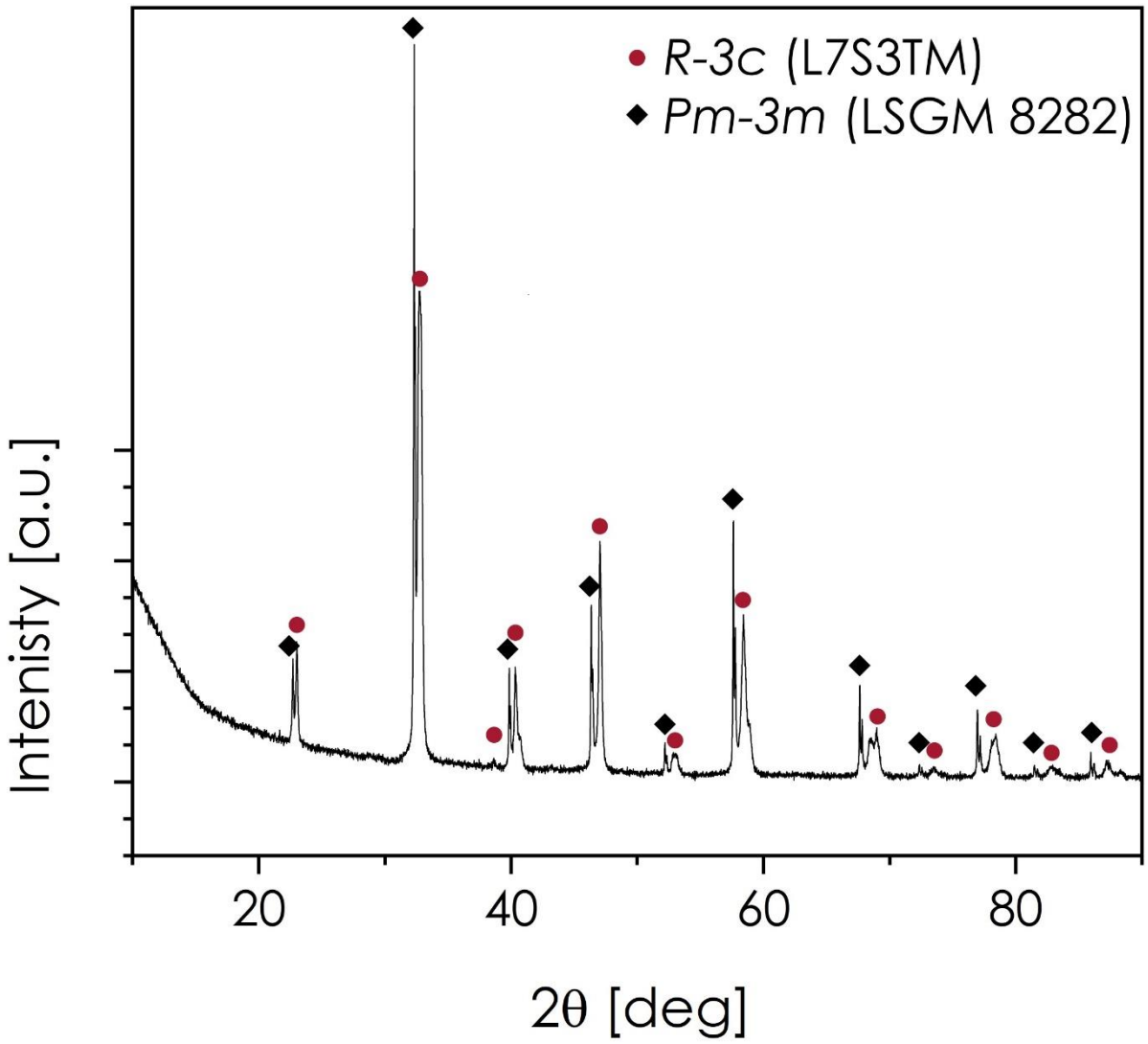

Figure S15. XRD diffraction pattern of the 50-50 wt.% pellet of mixed LSGM and L7S3TM powders after sintering for 2 h at 1100 °C.

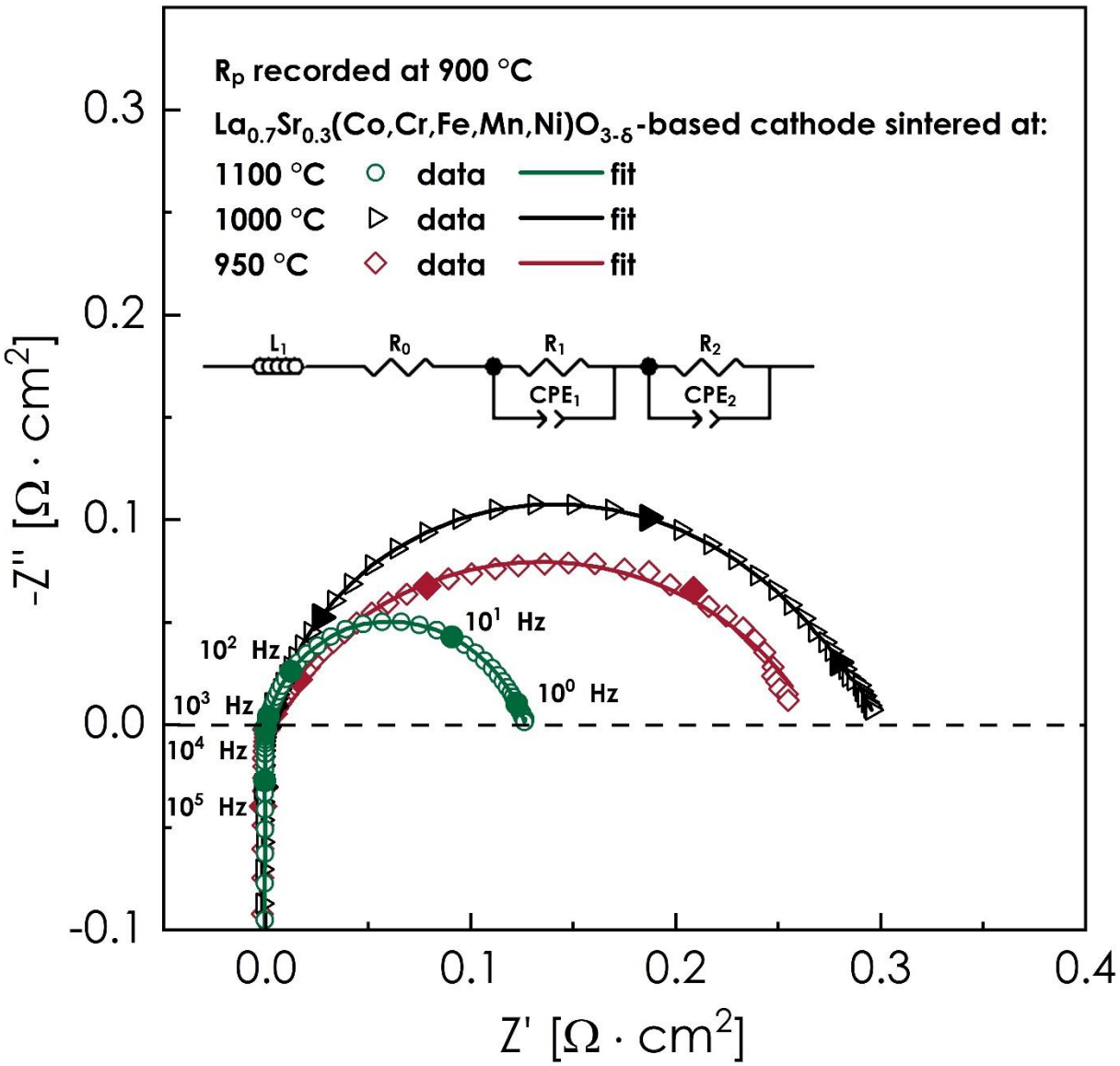

Figure S16. Impedance data recorded at 900°C for $La_{0.7}Sr_{0.3}(Co,Cr,Fe,Mn,Ni)O_{3-\delta}$-based cathodes sintered at 950 °C, 1000 °C and 1100 °C.

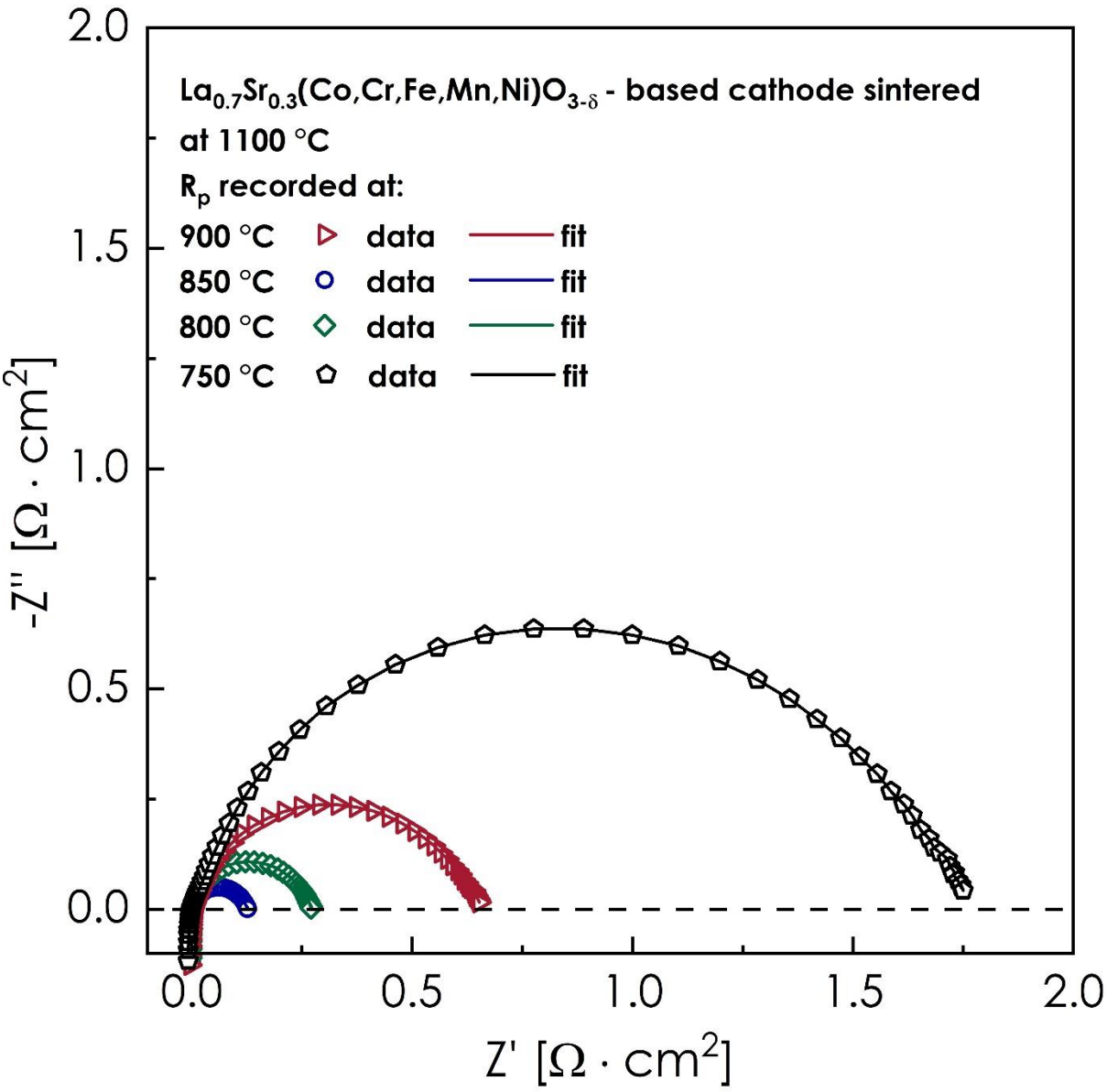

Figure S17. Exemplary results of the electrode polarization resistance measurements performed with the use of EIS.

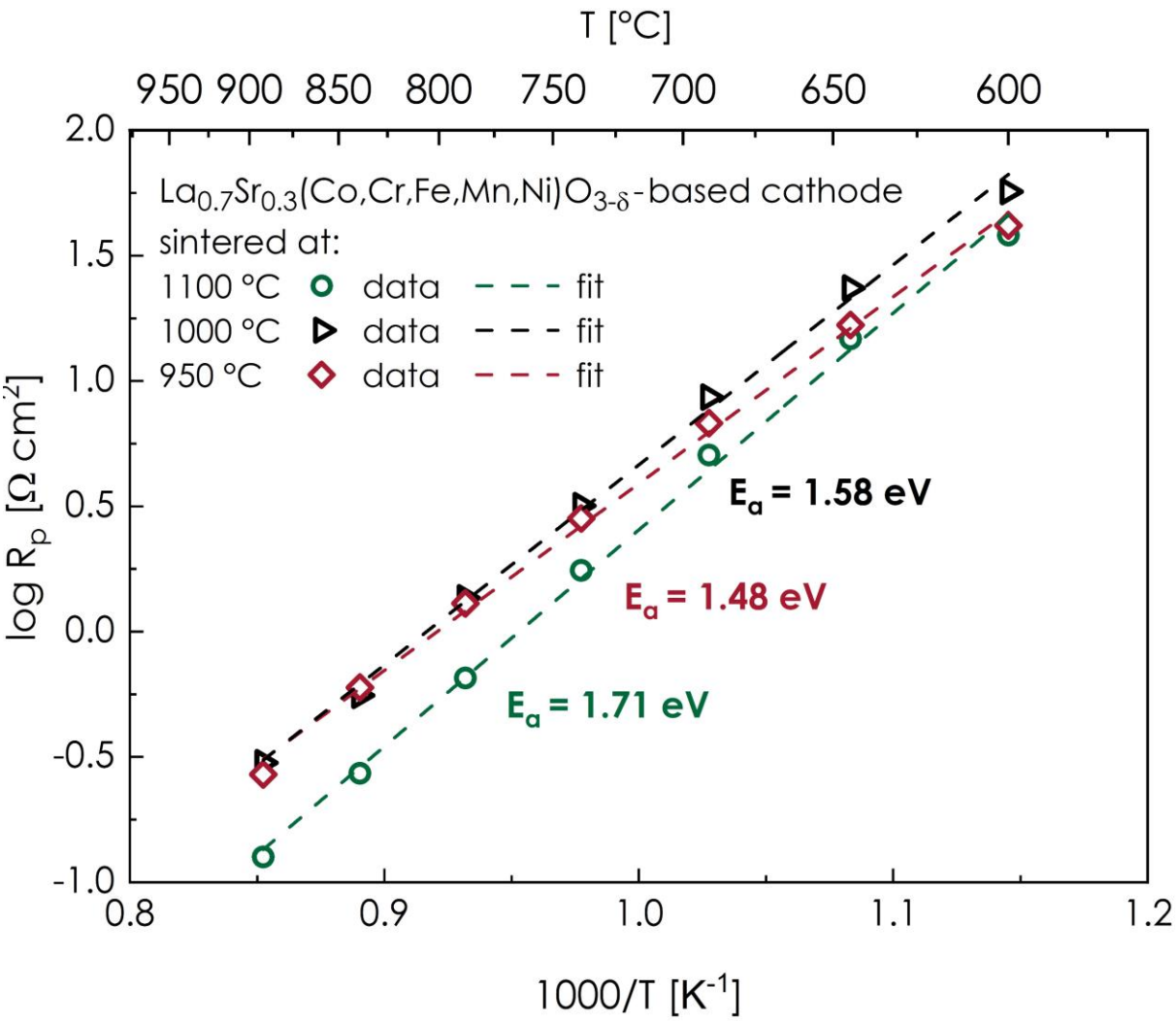

Figure S18. Temperature dependence of the total cathodic polarization resistance for $La_{0.7}Sr_{0.3}(Co,Cr,Fe,Mn,Ni)O_{3-\delta}$-based cathodes sintered at 950 °C, 1000 °C, and 1100°C.

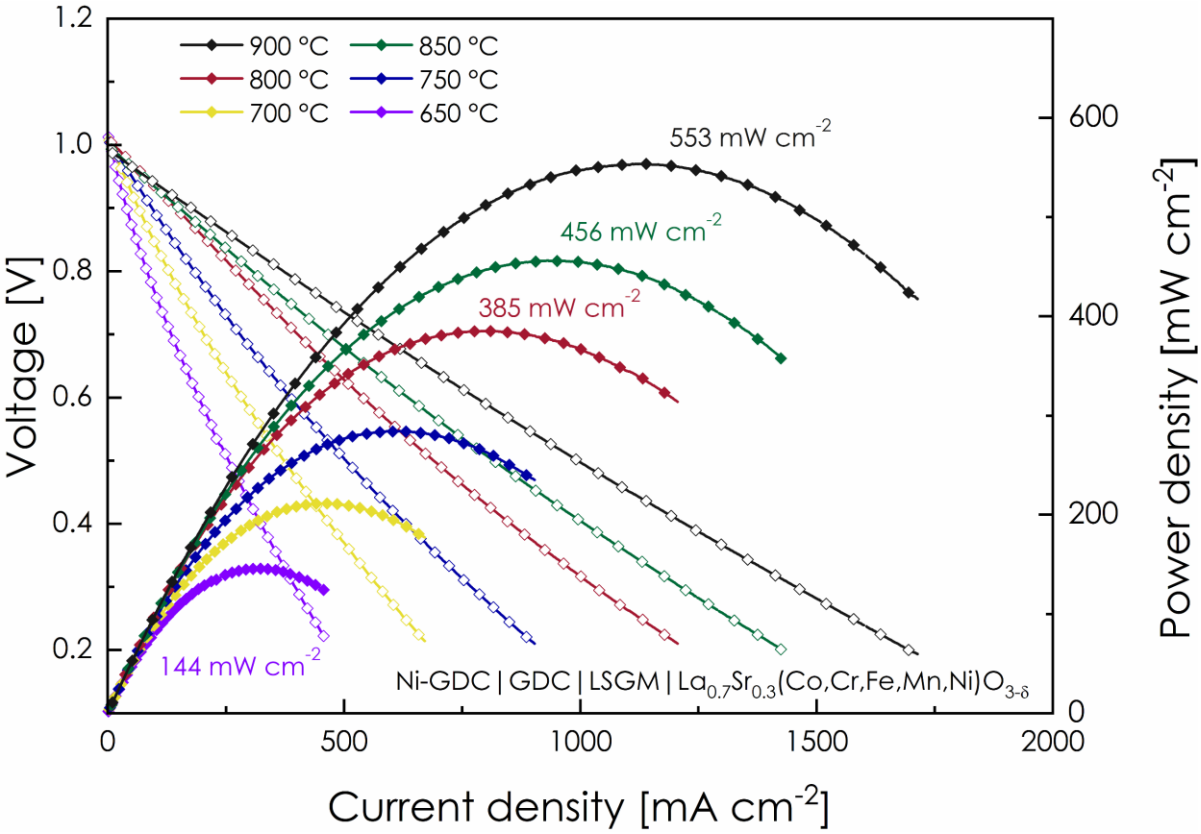

Figure S19. Current-voltage and power density curves recorded in 650-900 °C temperature range for Ni-GDC|GDC|LSGM|$La_{0.7}Sr_{0.3}(Co,Cr,Fe,Mn,Ni)O_{3-\delta}$ button-type fuel cell.